DEUTSCHES ELEKTRONEN-SYNCHROTRON DESY

DESY 88-027
MZ-TH/88-03
March 1988

SCALING BEHAVIOR AND VOLUME DEPENDENCE OF THE SU(2) TOPOLOGICAL SUSCEPTIBILITY

by

M. Kremer

Institut für Physik der Johannes-Gutenberg-Universität, Mainz

A. S. Kronfeld

Deutsches Elektronen-Synchrotron DESY, Hamburg

M. L. Laursen

Institut für Physik der Johannes-Gutenberg-Universität, Mainz

and

Niels Bohr Institute, Copenhagen

G. Schierholz

Deutsches Elektronen-Synchrotron DESY, Hamburg

and

Institut für Theoretische Physik, Universität Kiel

C. Schleiermacher

Institut für Theoretische Physik, Universität Hannover

U.-J. Wiese

II. Institut für Theoretische Physik, Universität Hamburg

ISSN 0418-9833

NOTKESTRASSE 85 · 2 HAMBURG 52

To be sure that your preprints are promptly included in the
HIGH ENERGY PHYSICS INDEX ,
send them to the following address (if possible by air mail) :

DESY
Bibliothek
Notkestrasse 85
2 Hamburg 52
Germany

DESY 88-027
MZ-TH/88-03
March 1988

ISSN 0418-9833

Scaling Behavior and Volume Dependence of the $SU(2)$ Topological Susceptibility

M. Kremer,[1] A.S. Kronfeld,[2] M.L. Laursen,[1,3,*] G. Schierholz,[2,4]
C. Schleiermacher,[5] and U.-J. Wiese[6]

[1]Institut für Physik der Johannes-Gutenberg-Universität,
D-6500 Mainz, F.R. Germany

[2]Deutsches Elektronen-Synchrotron DESY,
Notkestraße 85, D-2000 Hamburg 52, F.R. Germany

[3]Niels Bohr Institute
Blegdamsvej 17, DK-2100 Copenhagen Ø, Denmark

[4]Institut für Theoretische Physik der Universität Kiel,
D-2300 Kiel, F.R. Germany

[5]Institut für Theoretische Physik der Universität Hannover,
Appelstraße 2, D-3000 Hannover, F.R. Germany

[6]II. Institut für Theoretische Physik der Universität Hamburg,
Luruper Chausee 149, D-2000 Hamburg 50, F.R. Germany

March 4, 1987

Abstract

Previous computations of the topological susceptibility χ_t, using numerical simulations of lattice gauge theory, are extended in a number of ways. Most significantly, the statistical errors are now very small. The precision permits a discussion of finite volume and finite lattice spacing effects. Lattice spacing effects seem to be under control; we estimate the density of "lattice artifacts" and find that it vanishes in the (quantum) continuum limit of the Wilson action. Moreover, χ_t follows asymptotic scaling for $2.5 \leq \beta \leq 2.7$ and deviates only slightly therefrom for $2.2 \leq \beta \leq 2.5$. In intermediate volumes χ_t rises monotonically in the region $0.6 \leq z_t \leq 1.8$, where $z_t = La\chi_t^{1/4}$ is a dimensionless measure of the physical volume of the system. For $z_t \geq 1.8$ the susceptibility is constant, within statistical errors, yielding the value $\chi_t \overset{V=\infty}{=} [(38.7 \pm 0.2)\Lambda_{\rm lat}]^4$.

*permanent address Mainz

Table 1: Parameters of the simulations. The lattice size is always L^4, β_F and β_A are defined in eq. (2.8), below, and N_Q is the number of configurations for which the topological charge was computed. Typically, there were 15 update sweeps between configurations.

L	β_F	β_A	N_Q	L	β_F	β_A	N_Q
6	2.20	0.0	5500	10	2.60	0.0	1800
4	2.30	0.0	24300	12	2.60	0.0	2600
6	2.30	0.0	5000	14	2.60	0.0	120
8	2.30	0.0	20000	2	2.70	0.0	101000
10	2.30	0.0	1600	4	2.70	0.0	100000
4	2.40	0.0	11700	6	2.70	0.0	20000
6	2.40	0.0	3900	8	2.70	0.0	10000
8	2.40	0.0	12500	12	2.70	0.0	1100
10	2.40	0.0	19069	16	2.70	0.0	1800
4	2.50	0.0	9000	8	2.30	0.1	800
6	2.50	0.0	6100	8	2.30	0.2	900
8	2.50	0.0	3000	8	2.30	0.3	500
10	2.50	0.0	7000	8	2.70	−0.2	2500
12	2.50	0.0	3200	8	3.00	−0.5	2500

1 Introduction

In a previous publication we presented Monte Carlo calculations of the topological susceptibility in $SU(2)$ lattice gauge theory [1]. The present paper extends that work to a new value of the (Wilson action) coupling ($\beta = 2.7$), to the mixed fundamental-adjoint action, to several new lattice sizes, and — most importantly — to very high statistics. Table 1 summarizes the parameters of the simulations: typical ensembles now contain several thousand configurations, whereas in ref. [1] there were typically only several hundred. Of course, the number of configurations can be misleading: the relative statistical errors are more important, and they are now around a few per cent. In the past the statistical errors for the topological susceptibility, as well as for other observables, were such that they could obscure the effects of finite volume and nonzero lattice spacing. However, the present precision means that we are in a position to disentangle these effects. In particular, we can analyze the contribution of small scale fluctuations to the topological susceptibility.

$SU(N)$ nonabelian gauge fields are characterized by an integer-valued topological charge

$$Q = -\frac{1}{16\pi^2}\int d^4x \ \mathrm{tr}\{F_{\mu\nu}{}^*F_{\mu\nu}\}, \quad {}^*F_{\mu\nu} = \frac{1}{2}\epsilon_{\mu\nu\rho\sigma}F_{\rho\sigma}, \tag{1.1}$$

the so-called second Chern number in mathematical parlance. It arises because it is impossible, in general, to pick a global gauge condition without singularities in the gauge potential A_μ. The topological susceptibility,

$$\chi_t = \langle Q^2\rangle/V, \tag{1.2}$$

where V is the volume of spacetime, is an observable quantity measuring the role of topologically nontrivial gauge fields in the quantum gauge theory. It is also related to physics through the celebrated Witten-Veneziano formula [2],

$$\chi_t = \frac{f_\pi^2}{6}(m_{\eta'}^2 + m_\eta^2 - 2m_K^2), \tag{1.3}$$

in the large N limit. Using experimental values on the right-hand side of eq. (1.3) yields $(180\ \mathrm{MeV})^4$, and a value of χ_t in this ballpark — even in the $N = 2$ theory — is recognized as a quantitative resolution of the axial U(1) problem.

The original motivation for computing χ_t was to verify eq. (1.3). With our previous $SU(2)$ paper [1] and work in $SU(3)$ [3], one should view this issue as settled. The range of values reported, from $(261\ \mathrm{MeV})^4$ for $SU(2)$ [1] to $(231\ \mathrm{MeV})^4$ for $SU(3)$ [4], gives an indication of the N dependence. Because eq. (1.3) is derived in the large N limit, one should *not* expect exactly $\chi_t = (180\mathrm{MeV})^4$; also, the Monte Carlo estimates (in MeV) have statistical and systematic errors of string tension calculations, as well. Thus, although we will modify the $SU(2)$ result of ref. [1], the Witten-Veneziano formula is no longer the primary motivation for this article.

To compute the topological charge of a *lattice* gauge field, one must devise a lattice approximant to the right-hand side of eq. (1.1) [4]. Unfortunately, simple approximants have no topological significance [5] — they do not produce an integer for Q. The correct procedure is to reconstruct a fiber bundle [6]. Then one automatically obtains an integer, because the topological charge is a topological invariant, the second Chern number, of the bundle. In the nicest construction [7] the second Chern number can be computed combinatorically in $SU(2)$, making high precision simulations feasible. In these methods one must worry about dislocations, which are small scale fluctuations contributing to the susceptibility. In the two-dimensional CP^1 model these singularities even prevent determination of the susceptibility in the continuum limit [8], although in other two-dimensional models this is not necessarily the case [9]. We have examined the role of these fluctuations using a lattice action with plaquettes in the fundamental and adjoint representations: adjusting the adjoint coupling varies the density of small scale fluctuations. All indications lead to the conclusion that the density of dislocations vanishes in the (quantum) continuum limit of the Wilson action.

Every numerical simulation of field theory has systematic errors that arise because the simulation is done for a cutoff theory. The two cutoffs are the finite volume (infrared cutoff) and the nonzero lattice spacing (ultraviolet cutoff). Physically relevant numbers emerge only when the cutoff dependence can be controlled. For the infrared cutoff, it is comforting if the volume dependence reproduces theoretical formulae for (large volume) finite size effects. For the ultraviolet cutoff, control means that contributions suppressed by a power of $a\Lambda$ are numerically small,[1] or, equivalently in practice, that dimensionless ratios remain constant for some range of the bare parameters in the Lagrangian, i.e. a scaling window exists.

Simulations of lattice gauge theory are now at the point where, at least for the pure glue theory, one can accumulate enough computer time to examine these aspects in detail. The main aim of this paper is to initiate such a program using the topological susceptibility to study the cutoff dependencies. The topological susceptibility lends itself to such an analysis for a number of reasons. Unlike for the glueball mass or the string tension, no curve fitting is needed to obtain the susceptibility — one just measures Q and squares it, thus it is easier to attain small statistical errors. In any finite volume χ_t is a genuine observable: using an appropriate lattice approximant of the continuum charge, there is no need to normalize or renormalize. The topological charge is a nonperturbative quantity with contributions from all length scales. Finally, it is the *pure glue* susceptibility that enters eq. (1.3) [2], so we can with good conscience avoid a ghastly simulation with dynamical quarks. Also, the algorithm that we use [1], [7] is quite efficient in computer time. In short, the susceptibility is ideally suited to the type of study we have in mind.

The remainder of this paper is organized as follows. The reconstruction of the fiber bundle from a lattice gauge field has certain advantages, which are reviewed is sec. 2. This section also addresses the conceivable drawbacks due to lattice artifacts in some detail. In sec. 3 we present the raw results for the topological charge, including the mixed fundamental-adjoint action simulations. We then analyze the volume dependence and scaling behavior of the topological

[1] Here a is the lattice spacing and Λ is some physical scale.

susceptibility. Our results do not agree with refs. [10], [11], which determines the charge from "cooled" configurations. It has long been our feeling that this method removes some of the topological structure of gauge fields, and we present numerical evidence for this in the Appendix. Finally, sec. 4 provides some pointers for the next generation of numerical simulations.

2 Method

To assign a topology to a lattice gauge field $\{U_\ell\}$, one must reconstruct the relevant topological object, the principal bundle, by interpolating between the lattice points. For $SU(2)$ we use the algorithm of Phillips and Stone [7], which is the fastest available. We present no details of the algorithm here: interested readers are advised to read ref. [7]; a short summary and the details of our implementation on a hypercubic lattice are in ref. [1]. The probability P_Q for a configuration to have charge Q is (formally) given by

$$\mathsf{P}_Q = \frac{\int [dU_\ell]_Q \exp\{-S[U_\ell]\}}{\int [dU_\ell] \exp\{-S[U_\ell]\}}, \tag{2.1}$$

where the path integration in the numerator is restricted to the sector with topological charge Q. (N.B.: The P_Q are volume dependent.) The P_Q are directly determined in the numerical simulation, and furthermore they are observable quantities. Even though the statement is trivial, it is important to emphasize that accurate and precise determination of the P_Q is the fundamental objective.

For the moment, let us focus on the topological susceptibility χ_t, especially on its dependence on the lattice regulator. Because of its topological basis, the Phillips and Stone algorithm preserves the property

$$\nabla_\ell Q = 0, \tag{2.2}$$

where ∇_ℓ denotes group covariant differentiation with respect to the parallel transporter on the link ℓ. Hence the topological susceptibility is not (multiplicatively) renormalized. Other approaches [5],[12] to the topological susceptibility do not preserve eq. (2.2), and therefore face the difficult task of determining the renormalization factor nonperturbatively. However, even in the topological approach, ambiguities in the interpolation at the scale of the lattice spacing imply that the bare susceptibility χ_t^0 has the form

$$\chi_t^0 = \chi_t + C(a\Lambda)^{p_1} |\ln(a\Lambda)|^{p_2} + \cdots, \tag{2.3}$$

where χ_t is the *physical* susceptibility. Of course, a similar formula holds for any other physical observable. The crucial exponent in eq. (2.3) is p_1; if $p_1 < 0$ then regulator artifacts dominate the susceptibility, whereas if $p_1 > 0$ then χ_t^0 converges to the physical value in the continuum limit. The exponent p_1 is regulator dependent: it depends not only on the definition of topological charge, but also on the choice of lattice action.

The configurations responsible for $C \neq 0$ in eq. (2.3) are certain structures of size $\approx O(a)$ contributing to the topological charge. These unphysical small scale fluctuations are called *dislocations* [13]. In the continuum limit the physical topological susceptibility scales according to the asymptotic formula

$$\chi_t \propto \left[\frac{1}{a}\left(\frac{\beta}{2N\beta_1}\right)^{\beta_2/2\beta_1^2} \exp\left(-\frac{\beta}{4N\beta_1}\right)\right]^4, \tag{2.4}$$

where $\beta_{1,2}$ are the first two coefficients of the perturbative Callan-Symanzik β-function:

$$\beta_1 = \frac{11N}{48\pi^2}, \quad \beta_2 = \frac{17N^2}{384\pi^4}, \tag{2.5}$$

Table 2: Minimum action of the $Q = 1$ sector and fluxon action for various parameters in the adjoint action.

β_F	β_A	$\bar{S}_{\min}$	$\bar{S}_{\text{fluxon}}$
0.8	+0.1	9.6	9.6
1.0	0.0	12.7	12.0
1.2	−0.1	14.7	14.4
1.4	−0.2	15.9	16.8
1.8	−0.4	17.2	21.6

for $SU(N)$. On the other hand, the dislocations provide a contribution to χ_t^0 that scales as

$$\chi_t^0 - \chi_t \propto a^{-4}\beta^{p_3}\exp(-\bar{S}_{\min}\beta), \tag{2.6}$$

according to a semiclassical expansion [14] about the dislocation with minimum action $S_{\min} = \beta\bar{S}_{\min}$. By folding eq. (2.4) and eq. (2.6) together, one obtains

$$p_1 = 4(N\beta_1\bar{S}_{\min} - 1) \quad \text{and} \quad p_2 = 2\left(p_3 - \frac{N\beta_2\bar{S}_{\min}}{\beta_1}\right). \tag{2.7}$$

In the CP^1, or equivalently $O(3)$, σ-model in two dimensions one has the unhappy situation that $p_1 < 0$, and consequently the initial attempts to compute the topological susceptibility did not exhibit scaling [8]. In this case, Lüscher [14] computes $p_3 = -1$ and estimates $\bar{S}_{\min} \approx 6.69$, and the CP^n equivalent of eq. (2.7) yields $p_1 = -0.935$. In fact, the Monte Carlo data [8] reproduce eq. (2.6) with $\bar{S}_{\min} \approx 6.69$ very well [14]. Petcher and Lüscher [9] study CP^n models for $n > 1$, and they show that for an action improved to suppress small scale fluctuations, one can raise $\bar{S}_{\min}$ in the CP^2 model in order to obtain $p_1 > 0$. For such actions they find universal scaling of χ_t with the correlation length.

To investigate dislocations in $SU(2)$ gauge theory in four dimensions, we have turned to the mixed fundamental-adjoint action:

$$S = \sum_p \beta_F\left(1 - \frac{1}{2}\mathrm{tr}(U_p)\right) + \beta_A\left(1 - \frac{1}{4}\mathrm{tr}^2(U_p)\right). \tag{2.8}$$

For $\beta_A < 0$ (> 0) this action suppresses (enhances) dislocations, compared to the standard Wilson action ($\beta_A = 0$). Starting from a fixed smooth $SU(2)$ configuration with $Q = 1$, we have searched for quasistable configurations using the diffusion equation on the group manifold in the Euler approximation. Specifically, we replace iteratively the configuration $\{U_\ell\}$ by $\{U_\ell'\}$ obtained by

$$U_\ell' = \exp(-\epsilon\nabla_\ell S)U_\ell \tag{2.9}$$

with stepsize $\epsilon = 0.025$. The history of the diffusion is shown in fig. 1 for five choices of the couplings (β_F, β_A) with $\beta_F + 2\beta_A = 1$, i.e. with the same naive continuum limit. For each choice one can perceive two plateaus: the first, especially stable one corresponds to the instanton; the second, less stable one is the dislocation. Using the topological charge program we have verified that $Q = 1$ before and $Q = 0$ after the collapse of the dislocation. From this plot one can read off the value of the action for the dislocation, as collected in Table 2. Notice that even the Wilson action has $\bar{S}_{\min} > 12\pi^2/11 \simeq 10.77$, so that according to eq. (2.7) $p_1 > 0$. Furthermore, we note that for $\beta_A \geq -0.1$ the dislocation obtained in this way resembles a fluxon: the six plaquettes surrounding a specific link have a high action density, whereas the rest of the plaquettes have

negligible action density. (The fluxon itself is the extreme case where the six plaquettes have $\mathrm{tr}(U_p) = -2$.) This substantiates the claim in ref. [1] that

$$\bar{S}_{\min} \geq \bar{S}_{\text{fluxon}} = 12 \tag{2.10}$$

for the Wilson action. For $SU(N)$ the fluxon has $\bar{S}_{\text{fluxon}} = 24/N$ (Wilson action); using it as a guide one finds

$$p_1 = 4\left(\frac{11N}{2\pi^2} - 1\right), \tag{2.11}$$

which yields $p_1 = 0.458$ for $SU(2)$ and $p_1 = 2.687$ for $SU(3)$.

Let us now return to the probability distribution P_Q. In this language the lesson of the foregoing analysis is that the distribution is essentially unaffected by dislocations if the exponent $p_1 > 0$, as it indeed is for the Wilson action. Dislocations still contribute to the charge assigned to a given configuration, but any systematic tendency to broaden the distribution disappears in the continuum limit.

3 Results

This section discusses the results of the numerical simulations. Since sec. 2 indicates that dislocations are suppressed in the continuum limit of the Wilson action, we will generally not make the distinction between the bare and physical susceptibilities in this section.

For the sake of reference, Tables 3 and 4 display the distribution of topological charge in the most interesting simulations. The tables provide the number of times charge Q occurred in the course of the simulation. The errors (in parentheses) are determined from fluctuations in successive subensembles. The tables also list $\langle Q \rangle$ and $\langle Q^2 \rangle$, and $\chi_t^{1/4}/\Lambda_{\text{lat}}$.

Fig. 2 shows our Monte Carlo results for $a^4\chi_t$ in $SU(2)$ as a function of β. The $\bullet$'s represent simulations performed with the Wilson action, whereas the $\blacktriangle$'s and the $\blacksquare$'s were done for the mixed fundamental-adjoint action, eq. (2.8). For the mixed action we use $\beta = 4/g^2$ obtained from the one-loop expression [15]

$$\beta = \beta_F + 2\beta_A - \frac{5}{2}\frac{\beta_A}{\beta_F + 2\beta_A} \tag{3.1}$$

which is consistent with the scaling behavior in previous work [16], [17], as long as the one-loop term remains small. We estimate statistical errors by computing the standard error of the susceptibility of various sized subensembles. The resulting error bars are much smaller than the symbols. Our results agree with other topological methods [18], [19], [20], within the errors of those studies (our errors are neglible in comparison). The solid line represents the $\beta = 2.6$, $L = 12$ result extended to other values of β using the two-loop scaling formula, eq. (2.4).

The three $\blacktriangle$'s have $(\beta_F, \beta_A) = (2.3, 0.1)$, $(2.3, 0.2)$, and $(2.3, 0.3)$ which enhance dislocations by decreasing p_1 in eq. (2.3). These points do not agree with the Wilson action values: the dashed line through them indicates dislocation dominated scaling with $\bar{S}_{\min} = 9$, which is the $\bar{S}_{\min}$ for $(\beta_F, \beta_A) = (2.3, 0.2)$. The two $\blacksquare$'s have $(\beta_F, \beta_A) = (2.7, -0.2)$ and $(3.0, -0.5)$ which suppress dislocations by increasing p_1. Taking volume dependence, statistical errors in χ_t, and systematic errors in β — which matter for the $(\beta_F, \beta_A) = (3.0, -0.5)$ point — they agree with the Wilson action results.

Fig. 2 is not very useful because it is impossible to tell if the deviations from the two-loop scaling curve are due to scaling violations or to finite volume effects. However, the errors are small enough so that we can disentangle the two. Ideally one would like to compare a dimensionless measure of the physical volume, such as $z_t = La\chi_t^{1/4}$, to another dimensionless ratio of physical observables. Fig. 3 uses the two-loop Λ_{lat}-parameter because the scaling behavior of fig. 2 is so

Table 3: Topological charge distributions. Simulations are labelled by lattice size and β value. The entries are the number of configurations with charge Q with errors in parentheses.

Q	6^4 2.2	6^4 2.3	8^4 2.3	10^4 2.3	8^4 2.4	10^4 2.4
−16				1(1)		
−15				1(1)		
−14			1(1)	7(3)		1(1)
−13			5(2)	6(2)		2(1)
−12			11(3)	15(3)		3(1)
−11	1(1)		22(5)	12(5)		6(3)
−10	3(2)		52(5)	24(3)	1(1)	33(7)
−9	18(5)		96(11)	33(8)	1(1)	42(4)
−8	30(4)		158(13)	47(8)	6(2)	107(6)
−7	52(7)	3(2)	376(9)	60(6)	10(3)	270(13)
−6	93(10)	12(2)	551(20)	71(6)	41(8)	440(16)
−5	186(12)	48(6)	835(22)	67(4)	110(8)	760(34)
−4	320(15)	117(9)	1139(41)	93(8)	347(8)	1066(22)
−3	443(17)	288(24)	1556(36)	94(14)	729(28)	1585(31)
−2	570(29)	615(19)	1924(30)	96(11)	1434(37)	1960(38)
−1	712(14)	876(15)	2198(40)	116(10)	2174(33)	2266(55)
0	692(22)	1104(34)	2122(50)	113(8)	2494(37)	2214(53)
+1	643(20)	853(24)	2164(53)	94(11)	2220(56)	2214(57)
+2	562(19)	586(18)	1979(48)	99(11)	1539(37)	1868(48)
+3	458(25)	319(25)	1543(16)	84(11)	817(23)	1496(41)
+4	316(20)	103(14)	1207(31)	98(7)	385(18)	1051(25)
+5	181(11)	57(7)	834(28)	88(5)	136(15)	741(16)
+6	123(8)	12(4)	535(29)	60(5)	39(9)	464(27)
+7	55(6)	4(3)	331(21)	75(8)	10(3)	254(11)
+8	28(5)	3(2)	184(9)	53(6)	5(2)	117(15)
+9	7(2)		101(11)	29(6)	2(1)	54(6)
+10	4(2)		38(5)	27(5)		32(5)
+11	2(1)		24(5)	9(2)		15(4)
+12	1(1)		9(3)	13(4)		6(1)
+13			3(1)	4(3)		1(1)
+14			2(1)	4(2)		1(1)
+15				3(1)		
+16				0(1)		
+17				2(1)		
+18				1(1)		
$\langle Q \rangle$	0.007(43)	0.006(34)	0.000(22)	0.063(98)	0.062(12)	-0.017(26)
$\langle Q^2 \rangle$	9.692(168)	3.908(59)	12.905(139)	31.178(732)	4.238(86)	11.038(135)
$\chi_t^{1/4}/\Lambda_{\rm lat}$	37.601(163)	38.537(145)	38.962(105)	38.860(228)	37.961(193)	38.579(126)

Table 4: More topological charge distributions.

Q	8^4 2.5	10^4 2.5	12^4 2.5	12^4 2.6	12^4 2.7	16^4 2.7
-11			1(1)			
-10			1(1)			
-9			3(1)			
-8			4(2)			
-7		2(1)	18(5)			
-6		14(4)	37(6)	4(2)		1(1)
-5		46(9)	87(14)	7(2)		9(3)
-4	4(2)	138(13)	168(11)	22(5)		24(6)
-3	44(7)	396(19)	262(6)	102(10)	6(3)	68(7)
-2	180(11)	774(20)	335(14)	263(18)	39(6)	197(6)
-1	660(40)	1287(28)	403(12)	551(27)	205(10)	372(6)
0	1235(31)	1621(45)	441(17)	724(27)	572(17)	444(20)
$+1$	656(24)	1389(38)	498(17)	521(24)	228(12)	352(14)
$+2$	172(12)	798(18)	359(15)	282(17)	44(5)	202(11)
$+3$	43(9)	358(17)	278(13)	92(10)	6(2)	87(9)
$+4$	5(2)	126(12)	144(10)	26(7)		32(4)
$+5$	1(1)	35(6)	93(9)	5(2)		7(2)
$+6$		14(3)	43(3)	1(1)		4(3)
$+7$		1(1)	15(4)			1(1)
$+8$		0(0)	6(2)			
$+9$		1(1)	4(2)			
$\langle Q \rangle$	-0.005(26)	-0.009(24)	0.045(56)	-0.013(30)	0.030(31)	0.052(38)
$\langle Q^2 \rangle$	1.225(41)	3.319(62)	7.486(98)	2.402(80)	0.794(37)	2.911(126)
$\chi_t^{1/4}/\Lambda_{\rm lat}$	35.847(300)	36.793(172)	37.574(123)	36.442(303)	35.628(415)	36.975(400)

tantalizing, and in order to avoid the statistical error of another numerical simulation. If the nonuniversal terms in eq. (2.3) are negligible, and if two-loop scaling applies, the Monte Carlo data should lie on a smooth curve. For $\beta \geq 2.5$ the data do indeed lie on the dashed curve, drawn to guide the eye, as shown in fig. 4. In similar plots with other coefficients of β in the scaling law, for instance $\bar{S}_{\rm min}$, the Monte Carlo data at different β values do not lie on a universal curve on the sensitive scale of the vertical axis of fig. 4. This indicates that the constant C in eq. (2.3) does not dominate the bare susceptibility, even at $\beta \approx 2.3$.

Now consider the data for $\beta < 2.5$. Since the contribution of dislocations C seems to be small relative to the physical susceptibility, it is fair to use χ_t as a standard of mass, i.e. to define $\Lambda_{\rm lat}$ in the region $2.2 \leq \beta \leq 2.5$. By insisting that χ_t at distinct values of β match at equal physical volume, one arrives at fig. 5. Extrapolating to infinite volume on this plot, we obtain the estimate

$$\chi_t \overset{V=\infty}{=} [(38.7 \pm 0.2)\Lambda_{\rm lat}]^4, \tag{3.2}$$

where the error is purely statistical. Systematic errors are harder to estimate, but the hand tuning of the Λ-parameter, for instance, introduces at most 7%, the amount the $\beta = 2.3$ data shifts in moving from fig. 3 to fig. 5. Thus eq. (3.2) is an excellent measure of the susceptibility, in (almost) physical units. Unfortunately, neither other Monte Carlo simulations nor laboratory experiments provide a well accepted result for $\Lambda_{\rm lat}$, so we are reluctant to state $\chi_t^{1/4}$ in MeV; the reader is, however, welcome to insert his favorite value for $\Lambda_{\rm lat}$. Also, given the uncertainties of eq. (1.3) we do not wish to exploit it in order to predict $\Lambda_{\rm lat}$; avid enthusiasts of eq. (1.3) can insert 180 MeV, if they so choose.

The volume dependence of χ_t at intermediate z_t is also very interesting, especially in light of ref. [21]. In small and intermediate volumes it is possible to perform analytic calculations [21], and these results agree very well with Monte Carlo calculations [22] of glueball masses and 't Hooft electric flux energies. In the approach of ref. [21] instanton mediated tunnelling is neglected, i.e. $\chi_t = 0$. There are several indications that the approximations used in the analytic calculations break down near $z_0 = Lam_0 \approx 5$, where m_0 is the mass of the "0^+" glueball. (For reference with fig. 5 we note that $z_0 \approx 4.7 z_t$.) In particular, ref. [21] anticipates that instantons become important at $z_0 \approx 5$; a signal for the validity of this idea would be a sudden jump in χ_t near $z_0 \approx 5$ ($z_t \approx 1$). The numerical results do not seem to reflect this scenario. For $z_t > 1.5$, χ_t is more or less flat, which is fine, but there is no drastic suppression at small z_t. In fact we see a smooth rise from $z_t \approx 0.5$ to $z_t \approx 1.5$, and the data is very consistent at $z_t \approx 1$ — right where the jump ought to be.

Several remarks can reconcile the discrepancy between the ideas of ref. [21] and the results of fig. 5. Firstly, there is presumably some instanton mediated tunnelling even in small and intermediate volumes; it just turns out that the tunnelling does not affect the spectrum much. Hence, $\chi_t \approx 0$ for $z_0 < 5$ is probably too much of an idealization. Secondly, very rare tunnelling at *small* volumes leads to a surprisingly large susceptibility, simply because the volume factor in eq. (1.2) is small. For example, in the $L = 4$, $\beta = 2.7$ run, only 0.7% (none) of the configurations are in the one-(two-)instanton sector; indeed, the exceedingly small fraction of configurations with $Q \neq 0$ is reflected in the large statistical errors in χ_t, despite the large total number of configurations. Thirdly, although the effects of dislocations become more obnoxious if the physical susceptibility shrinks, the data do not support the hypothesis that dislocations with $\bar{S}_{\rm min} \approx 12$ dominate the bare susceptibility at low z_t. If this were the case, then the low β points should appear higher in fig. 3 than the high β points, whereas the data are the other way around. Finally, though, our low z_t results may just be inconclusive: at $L = 4$, say, the distinction between ultraviolet and infrared is probably too muddled.

We end our analysis with the nonperturbative β-function, as determined from the suscepti-

bility at two adjacent values of the coupling:

$$-\left.\frac{\partial \ln a}{\partial \beta}\right|_{(\beta_1+\beta_2)/2} = \frac{1}{\beta_1-\beta_2}\ln\frac{\chi_t^{1/4}a(\beta_1)}{\chi_t^{1/4}a(\beta_2)} \quad \text{at constant } z_t, \tag{3.3}$$

which is shown in fig. 6. To attain the same z_t for both values of β we interpolate $\chi_t^{1/4}$ linearly in z_t, if necessary. Fig. 6 also shows the β-function as determined from the string tension [23], which shows larger deviations from asymptotic scaling.[2] Note that the hump in fig. 6 is qualitatively consistent with the "dip" in $\Delta\beta(\beta)$, the shift in β needed for a factor-of-two scale change, seen in other simulations [25], although for χ_t the deviations from two-loop scaling are much, much smaller.

4 Conclusions

The introduction stressed that the primary motivation for this study was to understand the effects of ultraviolet and infrared cutoffs in numerical simulations of lattice gauge theory, using the topological susceptibility as a tool. In the ultraviolet we conclude that nonuniversal lattice artifacts are not a problem, that the topological susceptibility scales asymptotically, for $\beta \geq 2.5$, and that the deviations from such behavior are small in any case. In the infrared we conclude that there is a nontrivial volume dependence up to $z_t \approx 1.8$ (i.e. $z_0 \approx 8.5$); the volume dependence is not precisely in line with the anticipation of ref. [21], but the discrepency can be reconciled.

The results presented in this paper can be improved in perhaps three repects, should another order of magnitude in computer power become available. First, the very large volume estimate in eq. (3.2) ought to be confirmed by simulations at $L = 16$ to 20 at $\beta = 2.5$ and on even larger lattices at higher values of β. As it stands data in the asymptotic scaling regime are in an intermediate volume. Second, contact with ref. [21] should be made at larger values of L so that there is still a distinction between infrared and ultraviolet: $L = 8$ to 32 at $\beta = 3.1$ to 3.5 should suffice. Finally, the Callan-Symanzik β-function would be better determined by a finer scan in $\beta = 4/g^2$, designed to match the physical volume. Clearly such a program calls for a very large scale project, one which presumably also aims at the string tension, glueball masses, and other observables. Such a project could perhaps resolve the lack of universal scaling: unlike the topological susceptibility the other observables do not scale asymptotically in the present range of β. In the meantime, other workers in lattice gauge theory are reminded that χ_t is a well-defined, interesting observable that can be computed on any lattice geometry.

Appendix

There have been attempts to compute the topological susceptibility in SU(2) and SU(3) gauge theories using a method based on cooling [10], [11]. Cooling is a useful heuristic tool for understanding the structure of the QCD vacuum, but it always underestimates χ_t. In ref. [11] the method is used to extract the topological charge by computing a naive lattice approximant to $\int d^4x\ \mathrm{tr}\{F_{\mu\nu}{}^*F_{\mu\nu}\}$ after an empirically determined number of cooling sweeps. Instead of the diffusion method refs. [10], [11] use a much harsher method, equivalent to heat-bath updating at infinite β. Because the method is heuristic, it suffers from several theoretical drawbacks: one cannot prove that it is gauge invariant or that it has the correct continuum limit. The cooling method is not based on topology, so it does not yield integer values for Q. For smaller values this

[2] However, corrections for finite L effects, which may be sizable at $\beta = 2.7$ and 2.8, have not been performed in ref. [23] (F. Gutbrod, private communication). A global fit to the static $q\bar{q}$-potential with explicit scale breaking has been given in ref. [24], leading to a nonuniversal β-function.

can be artificially rounded to the nearest integer, but for larger charges, which naturally occur in large volumes, the identification becomes more and more ambiguous.

One aim of the cooling method is to eliminate the dislocations, yet if sucessful, it obviously eliminates small instantons as well. Even more striking, the cooling algorithm used in refs. [10], [11], can even miss large instantons. In fig. 7 we show the evolution of the action and those references' lattice approximant to $\int d^4x \ \mathrm{tr}\{F_{\mu\nu}{}^*F_{\mu\nu}\}$ during cooling. The starting configuration is the lattice instanton of ref. [26] with core diameter $6a$ on a 12^4 lattice. By construction it has $Q = 1$, and in practice both the algorithms of Lüscher and of Phillips and Stone yield $Q = 1$. Also, the staggered fermion matrix has a zero mode [26]. In summary, the configuration has the topological and physical structure of a semiclassical instanton surrounded by quantum fluctuations. Under the cooling algorithm of refs. [10], [11] it just dies. Notably, the diffusion equation, which cools more slowly, preserves the instanton (now with core diameter $3a$ on a 6^4 lattice, which might be *less* stable), as indicated by the solid line in fig. 7.

The net effect of these systematic effects is that the distribution obtained by the cooling method is much too narrow, and the susceptibility derived from it is a severe underestimate.

Acknowledgements

Computer time for program development and production runs was provided by DESY, the Niels Bohr Institute, the KFA Jülich, and the Universities of Berlin, Hamburg, Hannover, and Kaiserslautern. We have benefited from discussions with F. Brandstaeter, M. Lüscher, and M. Müller-Preußker. MLL and CS are grateful to R.D. Peccei for hospitality at DESY; CS and UJW thank P. Sauer for guidance and support. Finally, we thank F. Gutbrod and R. Sommer for sharing their results and views on the string tension calculations. Sylvester Stallone did not typeset this manuscript in LaTeX.

References

[1] A.S. Kronfeld, M.L. Laursen, G. Schierholz, and U.-J. Wiese, *Nucl. Phys.* **B292** (1987) 330.

[2] E. Witten, *Nucl. Phys.* **B156** (1979) 269;
G. Veneziano, *Nucl. Phys.* **B159** (1979) 213.

[3] M. Göckeler, A.S. Kronfeld, M.L. Laursen, G. Schierholz, and U.-J. Wiese, *Nucl. Phys.* **B292** (1987) 349; in preparation.

[4] For a recent review see A.S. Kronfeld, DESY report DESY 87-152, to appear in *Nucl. Phys.* **B** supplement *Field Theory on a Lattice*, edited by A. Billoire, et al.

[5] P. di Vecchia, K. Fabricius, G.C. Rossi, and G. Veneziano, *Nucl. Phys.* **B192** (1981) 392; *Phys. Lett.* **108B** (1982) 323.

[6] M. Lüscher, *Commun. Math. Phys.* **85** (1982) 29.

[7] A. Phillips and D. Stone, *Commun. Math. Phys.* **103** (1986) 599.

[8] B. Berg and M. Lüscher, *Nucl. Phys.* **B190** (1981) 412;
G. Martinelli, R. Petronzio, and M.A. Virasoro, *Nucl. Phys.* **B205** (1982) 255.

[9] D. Petcher and M. Lüscher, *Nucl. Phys.* **B225** (1983) 53.

[10] M. Teper, *Phys. Lett.* **171B** (1986) 81, 86.

[11] J. Hoek, M. Teper, and J. Waterhouse, *Phys. Lett.* **180B** (1986) 112; *Nucl. Phys.* **B288** (1987) 589.

[12] J. Smit and J. Vink, *Nucl. Phys.* **B284** (1987) 234; in *Lattice Gauge Theory 1986*, edited by H. Satz, I. Harrity, and J. Potvin (Plenum, New York, 1987); *Phys. Lett.* **194B** (1987) 433; Amsterdam preprint IFTA-87-7 (August 1987).

[13] B. Berg, *Phys. Lett.* **104B** (1981) 475.

[14] M. Lüscher, *Nucl. Phys.* **B200** (1982) 61.

[15] A. di Giacomo and G. Paffuti, *Nucl. Phys.* **B205** (1982) 313.

[16] G. Bhanot and M. Creutz, *Phys. Rev.* **D24** (1981) 3212.

[17] G. Bhanot and N. Seiberg, *Phys. Rev.* **D29** (1984) 2420.

[18] I.A. Fox, J.P. Gilchrist, M.L. Laursen, and G. Schierholz, *Phys. Rev. Lett.* **54** (1985) 749.

[19] Y. Arian and P. Woit, *Nucl. Phys.* **B268** (1986) 521;
P. Woit, *Nucl. Phys.* **B262** (1985) 284.

[20] G. Lasher, A. Phillips, and D. Stone, in *Quark Confinement and Liberation: Numerical Results and Theory*, edited by F. Klinkhammer and M.B. Halpern (World Scientific, Singapore, 1985).

[21] J. Koller and P. van Baal, CERN report TH.4897/87, to appear in *Nucl. Phys.* **B** supplement *Field Theory on a Lattice*, edited by A. Billoire, et al, and references therein.

[22] B. Berg, in *Lattice Gauge Theory 1986*, edited by H. Satz, I. Harrity, and J. Potvin (Plenum, New York, 1987);
B. Berg, A. Billoire, and C. Vohwinkel, *Phys. Rev. Lett.* **57** (1986) 400.

[23] R. Sommer, SCRI report FSU-SCRI-87-82.

[24] F. Gutbrod, *Z. Phys.* **C37** (1987) 143.

[25] A. Patel and R. Gupta in *Advances in Lattice Gauge Theory*, edited by D.W. Duke and J.F. Owens (World Scientific, Singapore, 1985) and references therein.

[26] I.A. Fox, M.L. Laursen, G. Schierholz, J.P. Gilchrist, and M. Göckeler, *Phys. Lett.* **158B** (1985) 332.

Figures

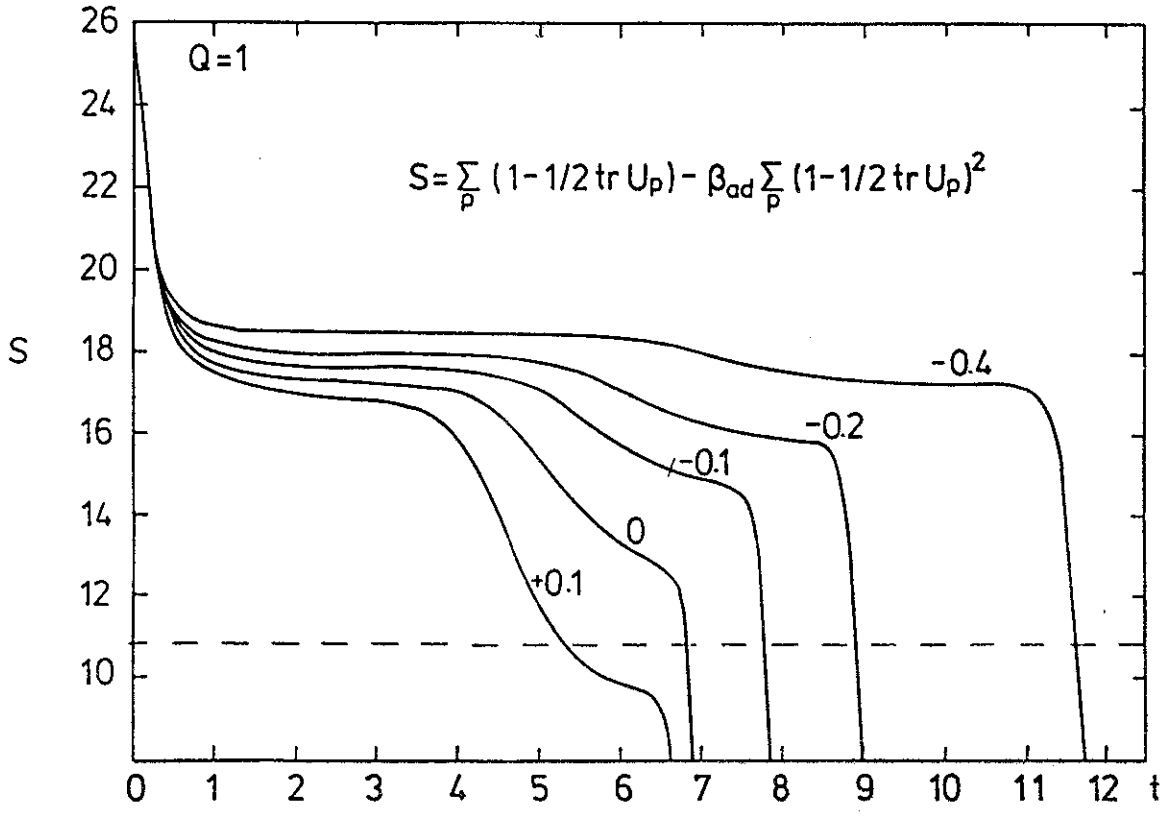

Figure 1: Cooling history of a smooth $Q = 1$ configuration. The value of the action S (defined in the figure) is plotted versus the time of diffusion. Only for $\beta_{ad} = +0.1$ is the dislocation plateau below the β-function value 10.77 (dashed line). All dislocations have Wilson action very close to $\bar{S} = 12$; after decay of the dislocation, the topological charge (using the Phillips-Stone algorithm) is $Q = 0$.

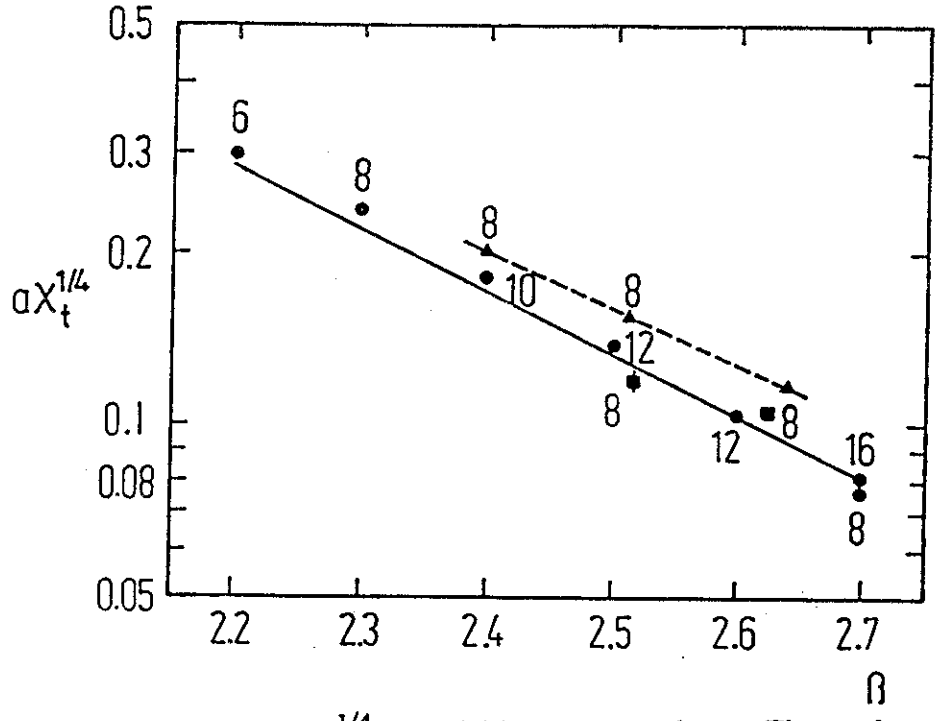

Figure 2: Topological susceptibility $a\chi_t^{1/4}$ in $SU(2)$ lattice gauge theory. The number next to the symbols are the lattice size L. • uses the Wilson action; for these points the errors are too small to plot. ▲ uses a mixed action that *favors* dislocations. ■ uses a mixed action that *suppresses* dislocations.

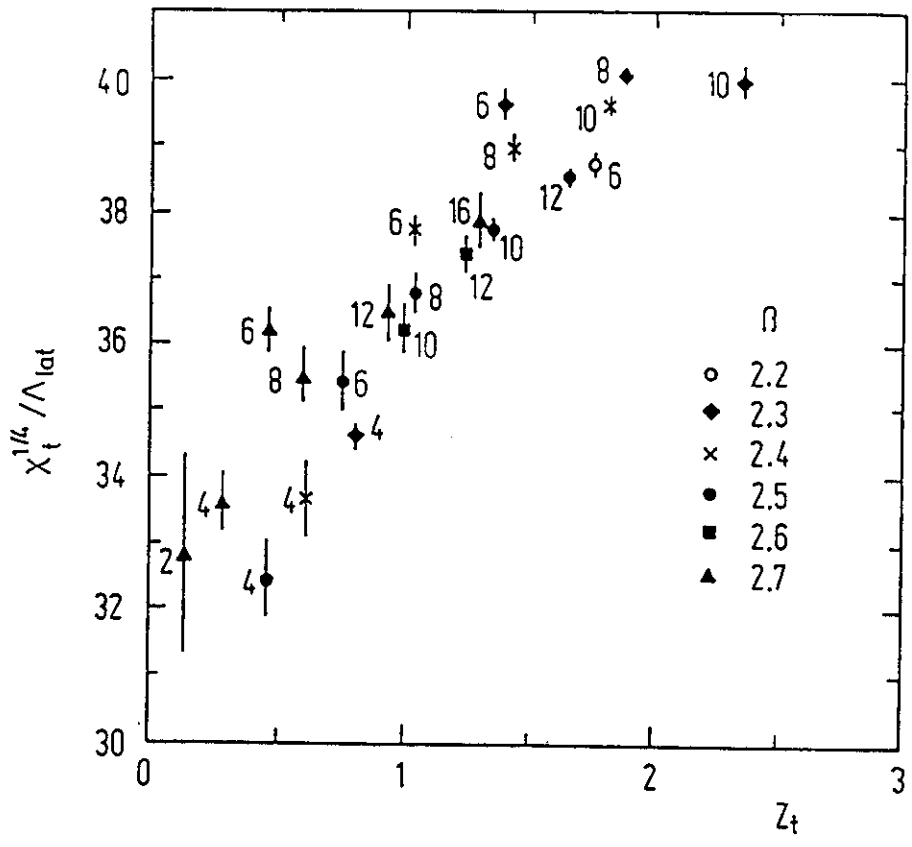

Figure 3: $\chi_t^{1/4}/\Lambda_{\rm lat}$ vs. z_t. Here $\Lambda_{\rm lat}$ is taken from the two-loop perturbative formula.

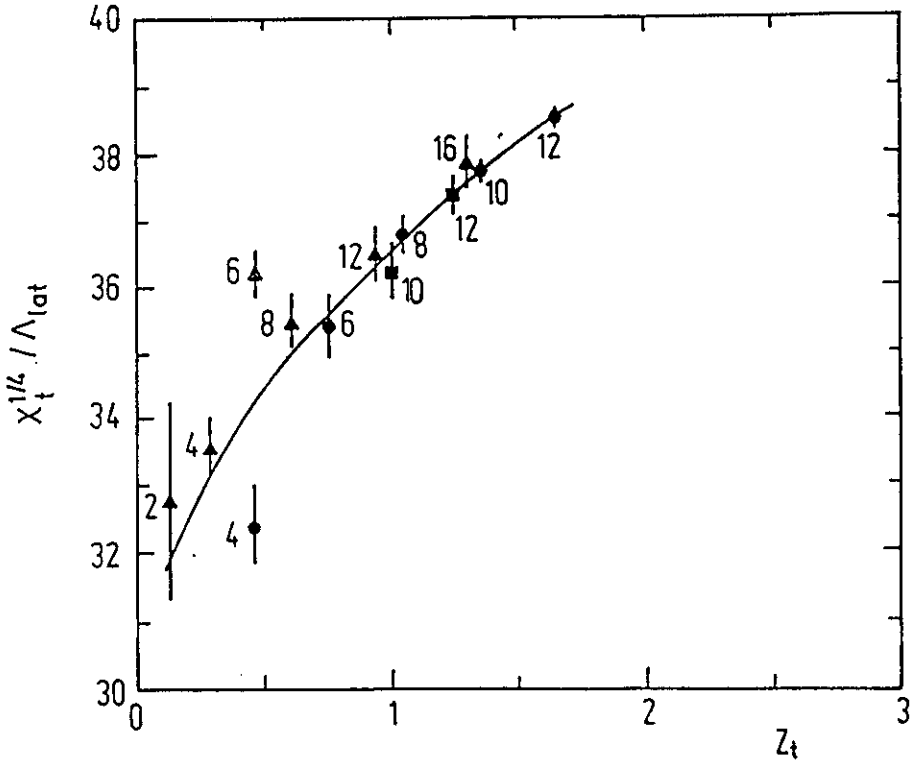

Figure 4: Same as fig. 3, but restricted to $\beta \geq 2.5$. The line emphasizes that the data lie on a universal curve (drawn to guide the eye).

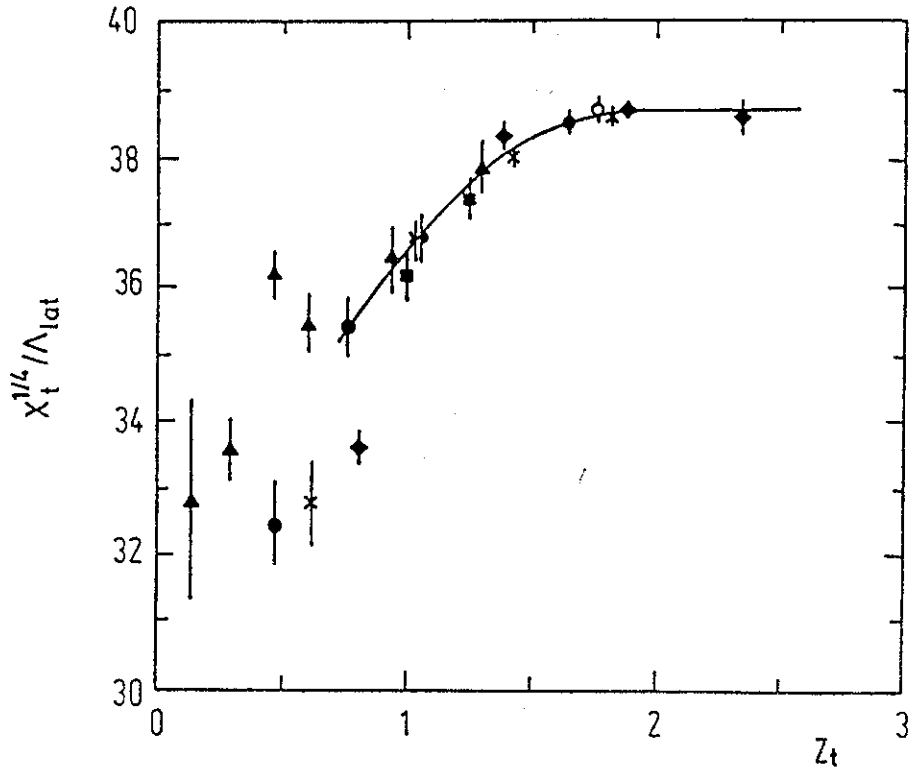

Figure 5: Same as fig. 3, but with Λ_{lat} adjusted, for $\beta = 2.3$ and 2.4, so that all data lie on a universal curve (drawn to guide the eye).

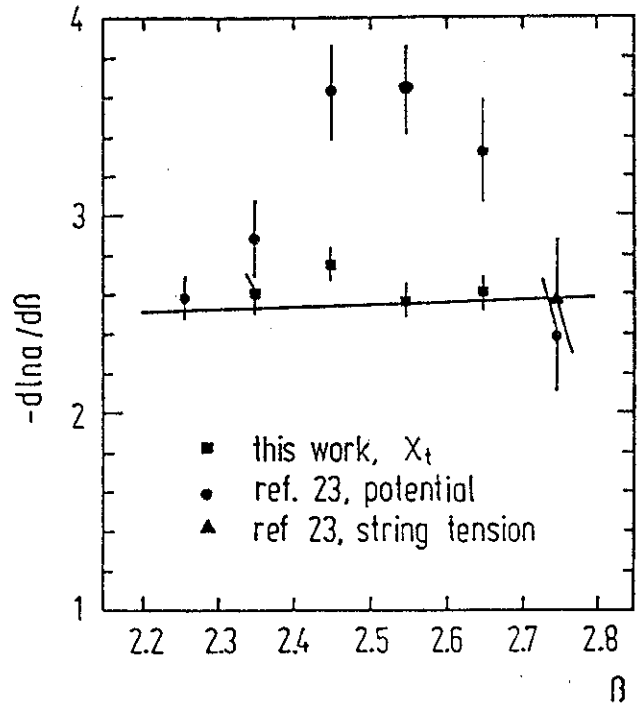

Figure 6: The nonperturbative β-function as determined by the topological susceptibility χ_t and the heavy quark potential [23]. Except at $\beta = 2.75$ the string tension extracted from the potential yields the same result.

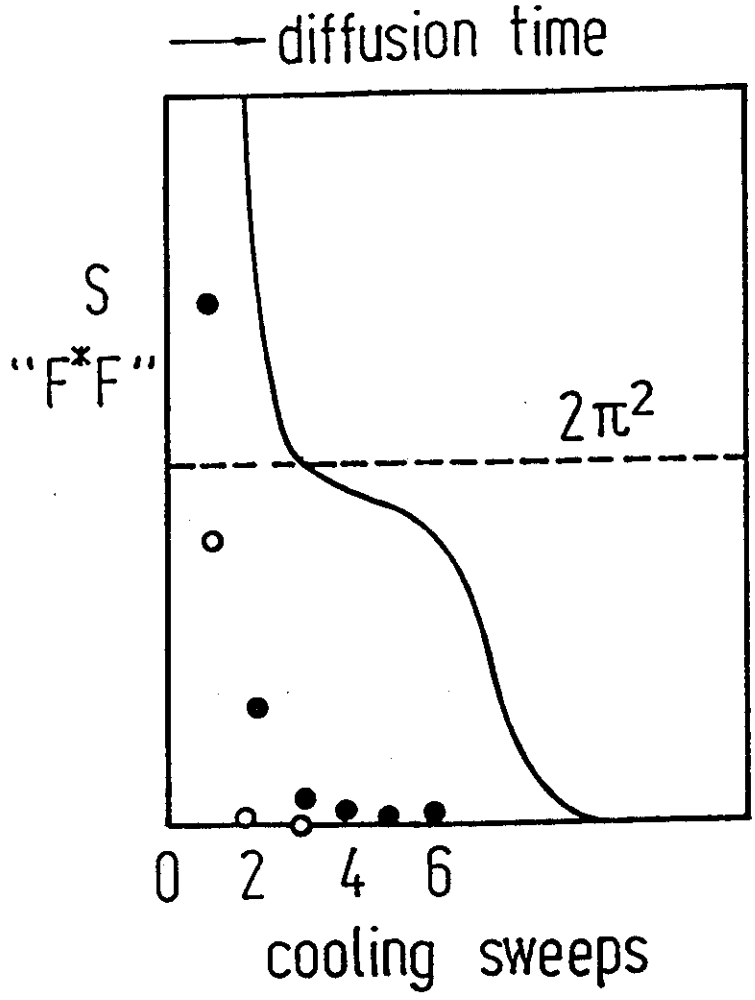

Figure 7: History of the configuration of ref. [26] during cooling. • shows the action and o the lattice approximant to the topological charge using the method of ref. [10], and [11], in units so that both are $2\pi^2$ for an exact instanton. The solid line shows the fate of this configuration using diffusion.